SUBATECH

Laboratoire de physique subatomique et des technologies associées

Unité Mixte de Recherche 6457
Ecole des Mines de Nantes, IN2P3/CNRS, Université de Nantes

PHOTON PHYSICS AT ULTRARELATIVISTIC-ENERGY HEAVY ION COLLISIONS (*)

Y. SCHUTZ

Rapport Interne SUBATECH 99-11

(*) Talk presented at 12th Indian Summer School RHIP 99. August 30- september 03 -1999, Prague, Czech Republic, (http//gemma.ujf.cas.cz/school)

ECOLE DES MINES DE NANTES

Adresse : Subatech - Ecole des Mines de Nantes
4, rue Alfred Kastler - La Chantrerie - BP 20722 - 44307 Nantes cedex 3
Tél. 02 51 85 81 00 - Fax 02 51 85 84 79 - http://www-subatech.in2p3.fr

Photon physics at ultrarelativistic-energy heavy-ion collisions

Yves Schutz
SUBATECH, *4 Rue Alfred Kastler F-44307 Nantes*

Abstract

Photons are discussed as potential probes of the dynamics of nucleus-nucleus reactions at ultrarelativistic energies. The signals conveyed by photons produced in the early partonic phase of the collision are explored. The discussion is illustrated by presently existing calculations which include photon production during the entire duration of the collision.

1 Introduction

One of the foremost challenges of modern nuclear physics consists in the experimental and theoretical investigation of nuclear matter under extreme conditions of temperature and density. Such extreme states of matter can be produced in the laboratory only by colliding heavy-ions at ultrarelativistic energies. At such high energies, which roughly correspond to center of mass energies of $\sqrt{s} > 100A$ GeV, the two colliding nuclei are viewed as two clouds of valence and sea partons (parton is the collective term for quark and gluon) which interact passing through each other, leaving in the mid-rapidity region a fireball of interacting quarks, antiquarks and gluons. If there is a sufficient number of interactions, the system may equilibrate and reach temperatures larger than the critical temperature ($T_c \approx 160$ MeV). At this temperature lattice Quantum Chromodynamics (QCD) predicts a phase transition for finite baryon-free nuclear matter, from quarks and gluons confined within hadrons to a plasma in which quarks and gluons are deconfined and move quasi-freely. By searching for the quark-gluon plasma (QGP) and exploring the physics of this new state of matter, ultrarelativistic heavy-ion collisions thus provide a unique tool to investigate the fundamental prediction of QCD that quarks can be deconfined (for a good starter see Reference [1]).

What is the structure of matter formed in heavy-ion collisions? Does the initial partonic system reach thermodynamical equilibrium? If so, at what temperature does the phase-transition occur? What is the order of the transition? Those questions belong to the open problems experiments are addressing. Three experimental programs benefitting from increasing available center-of-mass energy have been launched in order to seek for the deconfinement in dense and hot nuclear matter. With the earlier one at CERN SPS, Lead nuclei impinge on a fixed target at $\sqrt{s} = 17A$ GeV, which is expected to be sufficient to heat up baryon-rich matter at temperatures close to the critical temperature. So far, at this energy no firm evidence for the formation of a quark-gluon plasma has been demonstrated. The two later programs are still under construction: RHIC (Relativistic Heavy-Ion Collider) at Brookhaven (USA), will make collide by the end of 1999 Gold nuclei at $\sqrt{s} = 200A$ GeV and in 2005 LHC (Large Hadron Collider) at CERN will make collide Lead nuclei at $\sqrt{s} = 5.5A$ TeV. At these energies, nuclear matter is predicted to be transparent enough to form baryon-free nuclear matter heated up well beyond the expected phase-transition temperature. These energies finally ensure that enough time will be available for the formation of a plasma and its equilibration; it is estimated to amount to $3 - 5$ fm/c at RHIC energies and more than 10 fm/c at LHC energies.

To reach this experimental goal and evidence the formation of the new state of matter, one obviously needs first to select observables conveyed by probes which ideally are both sensitive to the new state of matter and capable of carrying the information to the detector without any perturbation. These criteria cannot be attained easily. First, because of the collision dynamics, matter spends fleetingly short times in the state of interest and passes continuously through different

thermodynamical states while producing the candidate probes. Once the particle is produced, it still has to escape from the medium without interaction before it can fly freely towards the detector. Electromagnetic particles, like real or virtual photons, offer solutions to this problem.

However, since there does not exist an universal probe, experiments will study several observables which may convey concurrently signatures of the formation of the quark-gluon plasma. This is the strategy of the experiments elaborated at RHIC and LHC around detector systems pointing at the mid-rapidity region for the detection of most of the heavy-ion reaction products.

Next I will briefly recall why photons are considered as a particularly interesting probe and how the heavy-ion collision evolves in time emphasizing the phenomena which can be explored using photons. I will then review which are the current predictions on photon production. I will end this lecture by discussing a few examples which extend the scope of photon physics beyond the measurement of just the energy spectrum.

2 Photons as probes

Any terrestrial or celestial matter can be best studied by analyzing its light spectrum because photons carry unperturbed information about the source in which they have been produced. In heavy-ion physics at energies around the Fermi energy, i.e., below the pion production threshold, photons already proved [2] to be a powerful probe of the history of the collision and well suited for the study of hot and dense nuclear matter. The same remains valid at ultrarelativistic energies although it becomes technically much harder to detect photons in an environment overwhelmed by hadrons. Indeed, at these energies pions are abundantly produced and it becomes extremely difficult to extract *direct* photons out of the bulk of produced photons mainly stemming from the radiative decay of neutral pions (typically beyond 80% of the background). Despite of this technical difficulty, the prime interest for photons remains strongly motivated by two facts:

- Photons are electromagnetically interacting particles, therefore their mean free path in the nuclear medium is expected to be quite large. Photons do not suffer a collision after production even in the densest matter and escape from the system without re-scattering.
- The photon spectrum and their production rate reflect the momentum distribution of matter constituents, which is governed by the (thermo)dynamical state of the system.

Hence, photons convey to the detector unperturbed information on the thermodynamical state of the medium at the moment of their production. The hardest photons accompanying the initial hard scattering and the subsequent parton cascade during the early stage of the heavy-ion collision, shed light on the formation of partonic matter and on the equilibration process. When the longitudinal momentum is damped into random motion, a typical softer photon spectrum is radiated, characteristic of the thermalized plasma. Still softer photons are emitted from the system while it cools down and hadronizes and can be used to study the thermodynamical state of hot hadronic matter. However, because of possible transverse expansion, one will observe these photons Doppler-shifted towards higher energies. The measured photon spectrum will integrate these radiations and only models including the photon production and the collision dynamics will help to disentangle the various origins. At variance with photons, hadrons do not decouple from the medium until late in the collision when the energy density is lower, and their final spectrum is influenced by their last scattering. Thus hadronic spectra are chiefly determined from the conditions at matter freeze-out.

Massive photons, which are detected as di-leptons, share with real photons similar interesting features. They are nevertheless produced with reduced cross-sections as compared to the photon cross-sections by a factor of the order α_e/α_s. They have, as well as di-photons [3], the additional advantage over single photons that that they carry an additional degree of freedom, the mass, that is invariant under Lorentz transformation, and is not affected by the transverse flow in the expanding plasma. Real and virtual photons convey thus complementary information and it will be rewarding to compare their spectra [4]. Indeed, photons are mainly produced through gluon Compton scattering and di-leptons through quark-antiquark annihilation. The two probes taken

together, hence provide valuable tools for probing the chemical composition of partonic matter during its early stages.

3 Heavy-ion collision dynamics

Since photons are produced at any stage of the collision evolution, a robust theoretical description of ultrarelativistic heavy-ion collisions involving the QCD-phase transition must be able to predict observables and help to disentangle signals linked to the collision dynamics on one hand and on the other hand those of interest linked to the hot partonic phase. A description of heavy-ion collisions at RHIC and LHC energies assumes that nuclear matter is quasi-transparent and that the Bjorken space-time scenario [5] of the collision is the appropriate picture: the two colliding nuclei traverse each other leaving in between baryon-free partonic matter which expands along the beam axis keeping a cylindrical symmetry. One considers usually two distinct stages:

1. The formation and pre-equilibrium stages during which a system of quasi-free partons is created and undergoes thermalization;

2. The equilibrium (or expansion) stage starts when local equilibrium is reached. It is characterized by an initial temperature and time. The system consisting of partons, or below the critical temperature of hadrons, expands and cools down to the freeze-out temperature.

The two stages are also distinct in the way they are theoretically modeled. In the first one the dynamics of the system is described at a microscopic level as colliding partons, and in the second the system is described at a macroscopic level by the equations of hydrodynamics. A third and ultimate stage, but with no immediate interest for the study of hot nuclear matter, starts when the size of the system is larger than the mean-free path of hadrons which then stream freely towards the detectors. The conventional representation of such a scenario is illustrated by Figure 1. We shall now look into the details of the two stages of interest.

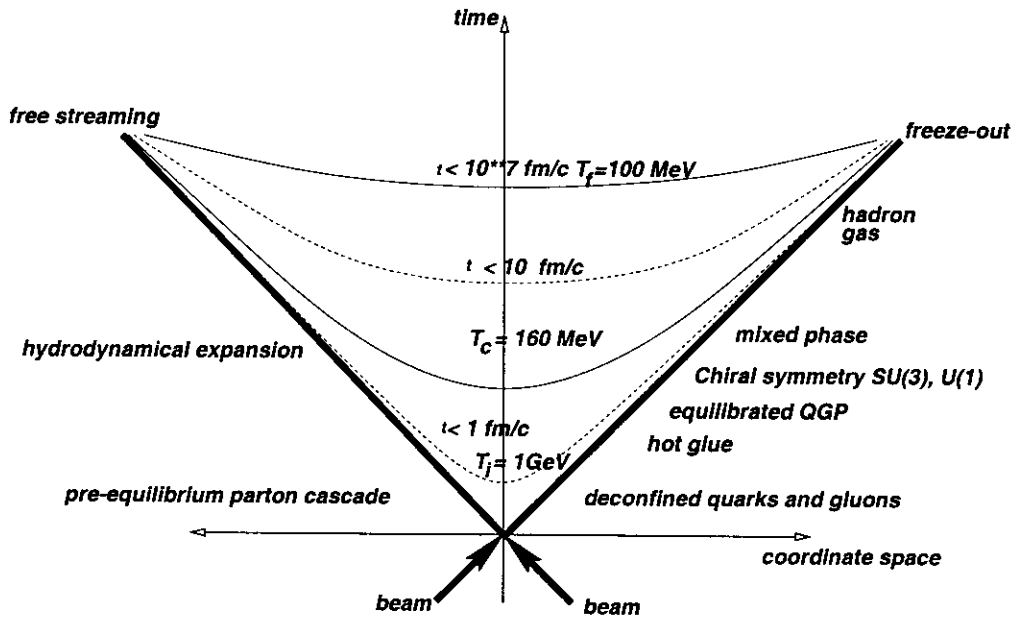

Figure 1: *Bjorken space-time scenario for heavy-ion collisions. The two Lorentz flattened nuclei collide at time zero, traverse each other leaving in between baryon-free matter consisting of quasi-free partons which evolves according to the equations of hydrodynamics. The parabola indicate constant proper times defined as the local time τ in the rest frame of any fluid element (for a cylindrically symmetric expansion, $\tau^2 = t^2 - z^2$).*

3.1 Pre-equilibrium phase

The two Lorentz-contracted impinging nuclei traverse each other with only little interaction and deposit part of their kinetic energy to heat up the central rapidity region. Hard (momentum scale of several tens of GeV/c) and semi-hard (momentum scale of a few GeV/c) scattering among partons liberate partons from the individual confining nucleons. Fast partons promptly escape the system before they have a chance to make a collision with other partons. This results from the short duration of the formation phase, a few tenth of fm/c, compared to typical strong-interaction times of 1 fm/c. They materialize as an observable jet (a jet refers to a collimated collection of hadrons resulting from the hadronization of partons). However they may loose energy while traversing the dense partonic medium which results in a jet quenching and a broadening of the jet momentum in the transverse direction (see section 6). The semi-hard scattered partons form, in the region in-between the two fast traversing nuclei, dense matter consisting of quasi-free quarks and gluons [6]. Because of the low transverse momentum scale (a few GeV/c) their final state is referred to as mini-jets (not resolvable as distinct jets). If the partons experience a high enough collision rate, a system in local thermal equilibrium is formed, chemical equilibrium will probably be reached only later.

At energies $\sqrt{s} > 100A$ GeV, the transverse momentum transfer in each nucleon-nucleon collision is larger than the QCD scale ($\Lambda_{QCD} \sim 200$ MeV) and the individual partons inside a nucleon can be resolved. Therefore the formation and pre-equilibrium phases can be described at the parton level. Perturbative QCD applies and partons are the elementary constituents of the interaction. The hard scattering of valence and sea partons confined in nucleons which occur during a formation phase are described in models like NEXUS [7] or HIJING [8]. Following this formation phase, the pre-equilibrium phase is described by the dynamics of partons as a cascade of freely colliding particles (e.g. Parton Cascade Model [9] or VNI [10]). The main purpose of these cascade-type models is to explore the range of possible initial conditions of equilibrated partonic matter that may occur in the heavy-ion collision. Such calculations include the parton structure functions modified through nuclear effects: initial state interaction between partons and beam nucleons which smears the initial transverse energy of partons; nuclear shadowing which describes the depletion of low fractional momentum partons inside the nucleus; soft final state interactions of produced partons with spectator beam nucleons which broaden the initial transverse energy of the produced partons.

Once partons are in equilibrium, i.e., isotropically distributed in phase-space with equal slopes of transverse and longitudinal momentum distributions, the initial conditions for a macroscopic description of the subsequent temporal evolution of the system can be defined in terms of thermodynamical variables like temperature, chemical composition, fugacity ... Typical values, depending on models and assumptions, predict that the system could have equilibrated at proper time $\tau_i = 0.4 - 0.7$ fm/c and could reach temperatures as high as $T_i = 400 - 800$ MeV at RHIC energies and $\tau_i = 0.2 - 0.5$ fm/c, $T_i = 700 - 1000$ MeV at LHC energies. These values will, among others, strongly influence the photon production rate.

3.2 Equilibrium phase

Beyond the point at which the system achieves kinetic equilibrium, the subsequent expansion can be described by the equations of hydrodynamics until constituents cease interacting. This is estimated to occur at freeze-out temperatures of the order of $T_f \approx 100$ MeV. In Bjorken's hydrodynamic model the space-time evolution of the system is described as an one dimensional expansion, the system being viewed as a cylinder which expands along the longitudinal direction (see the center-of-mass representation in Figure 1). The dynamics of the system, considered as an ideal fluid and modeled by a relativistic field, can then be specified by the thermodynamical variables, energy density, pressure, temperature, and equation of state, as a function of proper time. The system is driven toward chemical equilibrium, on a longer time scale than the one to reach thermal equilibrium, by the two-body reactions: $gg \leftrightarrow q\bar{q}$ and $gg \leftrightarrow ggg$.

The thermodynamical properties of the system are described by an equation of state for an ideal gas of massless non-interacting particles [11] until the system has cooled down to the critical

temperature, $T_c \approx 160$ MeV. The system then enters the hadronization phase described by an equation of state for an ideal gas which includes all known hadrons. Depending on the order of the transition, the system may spend some time in a mixed phase where the quark-gluon plasma coexists with the hadron gas. It is estimated that the duration of the quark-gluon plasma ranges between 3 and 5 fm/c at RHIC energies and lasts as long as 10 fm/c at LHC energies. Important quantities for the photon production rate are the chemical composition of the quark-gluon plasma, the particle multiplicity and the duration of the various phases. Calculations [11] indicate that per rapidity unit about 1600 particles are produced at RHIC energies and 8000 at LHC energies in the central rapidity region. Moreover it is found that gluons clearly outnumber quarks (Figure 2). In addition, because perturbative cross sections for gluon-gluon interaction are larger than the ones for quark-quark and quark-gluon scattering, probably gluons equilibrate earlier than quarks and form an initial *hot glue* with temperature larger than the one of the later thermalized quark-gluon plasma [12]. This feature also strongly influences the photon production.

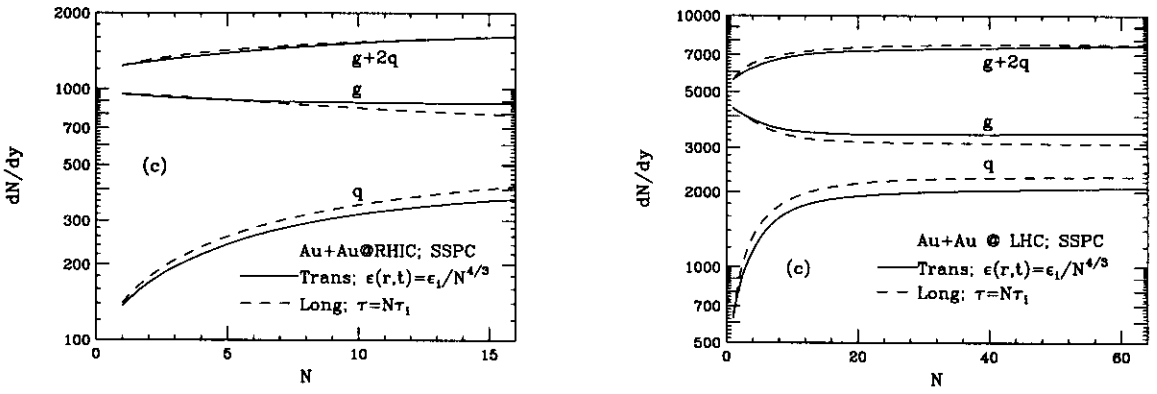

Figure 2: *Evolution during the equilibrium phase until hadronization, of the parton multiplicity calculated within the hydrodynamic model with (solid curves) and without (dashed curves) transverse flow for an ideal gas of massless non-interacting particles. From Reference [11].*

4 Photon production

We already know that photons are produced at any stage of the ultrarelativistic heavy-ion collision, from the early partonic phase through hard scattering among partons, to the late hadronic phase through hadron scattering. Those photons, which are of interest for the study of hot nuclear matter, will be referred to as *direct photons*. Another class of photons, the *decay photons*, will be emitted late in the collision through the radiative decay of the abundantly produced neutral mesons, mainly pions, once freeze-out is reached. This source of photons will outshine the sources of direct photons and therefore represents the major, but solvable, technical difficulty in the study of hot nuclear matter through the observation of its electromagnetic emission spectrum.

The direct photon spectrum as it will be measured, corresponds to the integration of the photon production rates over the space-time evolution of matter formed during the heavy-ion collision and therefore over the thermal and chemical history of the system:

$$E_\gamma \frac{dN_\gamma}{d^3p_\gamma} = \left(\sum_{N_1,N_2} E_\gamma \frac{dN_\gamma^{N_1,N_2}}{d^3p_\gamma} \right)_{Hard} + \left(\int d^4x E_\gamma \frac{dN_\gamma}{d^4x d^3p_\gamma} \left[T(x), u^\mu(x), \lambda_i(x) \right] \right)_{pre+QGP+hadron}, \quad (1)$$

where the first term represents the photon production through hard scattering, decomposed into a sum of the rate from binary nucleon-nucleon collisions. The second term includes all subsequent productions through semi-hard parton-parton scattering during the pre-equilibrium and equilibrium phases, and the production through hadrons scattering. $T(x)$ is the temperature field, $u^\mu(x)$

the 4-velocity field, and $\lambda_i(x)$ the fugacity of the interacting particles. The time evolution of these quantities is described by models as discussed in the previous sections. We shall consider the photon production separately in the various phases.

4.1 Pre-equilibrium photons

4.1.1 Formation

At formation time, photons are produced through hard and semi-hard parton scattering. Following the factorization theorem of QCD the cross-section for the scattering among two nucleons, N_1 and N_2, can be written in terms of elementary scattering among the partons, i, j:

$$\begin{aligned} N_\gamma^{N_1 N_2} &= \sum_{i,j} \int dx_i dx_j F_{i/N_1}(x_i, Q^2) F_{j/N_2}(x_j, Q^2) \\ &\times \left[\sigma_{i,j} + \alpha_s\left(Q^2\right) \sigma_{i,j}^{(1)} + \alpha_s^2\left(Q^2\right) \sigma_{i,j}^{(2)} + ... \right]. \end{aligned} \tag{2}$$

The $F_{i/N}(x_i, Q^2)$ in Equation (2) describe the probability to find a parton i with fractional momentum x_i inside a projectile nucleon. It is a function of the momentum scale Q^2 that characterizes the hard process. This distribution, including the in-medium quark and gluon shadowing at small fractional momentum, cannot be calculated within perturbative QCD and relies on parametrizations deduced from the data [13] and on the evolution equations for the Q^2 dependence [14]. The second factor represents the cross section for parton-parton scattering, leaving a photon in the final state, expressed as a sum of terms at the order $\alpha_s^{(n)}$. This factor is calculable provided Q^2 is large enough so that $\alpha_s(Q^2)$ is small. The dominant photon-production mechanisms are quark-antiquark annihilation ($q\overline{q} \to g + \gamma$) and gluon Compton-scattering ($g + q(\overline{q}) \to q(\overline{q}) + \gamma$). The cross-sections for these processes, calculated within perturbative QCD, have been checked against $p\overline{p}$ data [15]. The production in pA and AA reactions is then simulated by decomposing the collision into binary nucleon-nucleon collisions [8].

4.1.2 Pre-equilibrium

In the thermalizing partonic system formed by initial semi-hard scattering, the total photon production rate can be calculated as the incoherent sum of the rates in elementary processes of type $1 + 2 \to 3 + \gamma$ and with amplitude $\mathcal{M}$:

$$\begin{aligned} N_\gamma^{1+2\to 3+\gamma} &= \mathcal{N} \int \frac{d^3p_1}{2E_1\left(2\pi\right)^3} \frac{d^3p_2}{2E_2\left(2\pi\right)^3} f_1\left(E_1\right) f_2\left(E_2\right) \left(2\pi\right)^4 \delta\left(p_1 + p_2 - p_3 - p_\gamma\right) \left|\mathcal{M}\right|^2 \\ &\times \frac{d^3p_3}{2E_3\left(2\pi\right)^3} \frac{d^3p_\gamma}{2E_\gamma\left(2\pi\right)^3} \left[1 \pm f_3\left(E_3\right)\right], \end{aligned} \tag{3}$$

where the δ function ensures momentum and energy conservation, the f_i are the appropriate phase-space distributions of the particles involved in the process and $\mathcal{N}$ is a normalization factor. The total amplitude of the QCD-photon production can be calculated from the imaginary part of the retarded photon self-energy [16, 17]. Although the system has not yet reached thermal equilibrium one uses the concept of temperature to describe the average transverse momentum of the colliding partons. The photon self-energy can be approximated by carrying out a loop expansion known as the HOT THERMAL LOOP expansion (Figure 3). The imaginary part is then calculated from diagrams obtained by the cut technique applied to the Feynman diagrams of Figure 3. Among the possible cuts one retains only those which give rise to physical processes contributing at the order $\alpha_e \alpha_s$.

During the thermalizing phase the system is assumed to behave as an ideal gas which constituents are thermally distributed in phase-space according to Fermi-Dirac (quarks) or Bose-Einstein (gluons) distributions:

$$f_{q,\overline{q}(g)}\left(E\right) = \frac{\lambda_{q,\overline{q}(g)}}{\lambda_{q,\overline{q}(g)} \pm \exp\frac{E}{T}}, \tag{4}$$

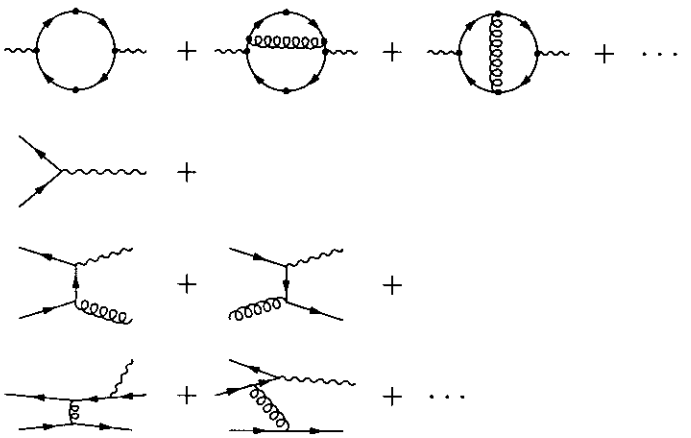

Figure 3: *Two-loop expansions of the photon self-energy to calculate the production of* QCD *photons. The photon production rate is proportional to the imaginary part which is obtained by cutting the Feynman diagrams in the top part of the figure. The physical processes are: (second line) the in-vacuum forbidden annihilation process with the emission of a single photon ($q\overline{q} \to \gamma$); (third line) Compton ($qg \to \gamma q$) and annihilation ($q\overline{q} \to \gamma g$) processes; (fourth line) bremsstrahlung processes ($qq(\overline{q}, g) \to \gamma qq(\overline{q}, g)$) and annihilation processes after scattering ($qq(\overline{q}, g) \to qq(\overline{q}, g)$ followed by $q\overline{q} \to \gamma$). From Reference [20].*

where the $\lambda's$ represent the fugacities. Considering only one-loop terms, QCD Compton and annihilation processes are the leading-order contributions for direct photon production:

- Compton process :

$$\begin{aligned} g+q &\rightarrow \gamma+q \\ g+\bar{q} &\rightarrow \gamma+\bar{q} \end{aligned}$$

The associated photon production rate evaluated from Equations (3) and (4) in the case where the photon energy is large ($E_\gamma \gg T$) is [18] :

$$\frac{E_\gamma dN_\gamma}{d^3p_\gamma d^4x} = \frac{2\alpha_e\alpha_s}{\pi^4}\sum_f \left(e_f^2\right)\lambda_q\lambda_g T^2 \exp\left(-\frac{E_\gamma}{T}\right)\sum_{n=2}^{\infty}\frac{(-\lambda_q)^n}{(n+1)^2}\ln\left(\frac{4E_\gamma T}{k_c^2}+\frac{1}{2}-C\right). \quad (5)$$

where e_f is the charge of quark summed over flavor f ($\sum_f \left(e_f^2\right) = 5/9$ for u and d quarks). The logarithm factor is introduced [19] to describe the infrared behavior with a cut-off parameter, k_c, which limits the four-momentum transfer and is related to the thermal mass of quarks in the medium ($k_c^2 = 2m_{th}^2 = 4\pi\alpha_s/3T$); $C = 0.57721$ is the Euler-Masheroni constant..

- Annihilation process :

$$\begin{aligned} q+\bar{q} &\rightarrow \gamma+g \\ q+\bar{q} &\rightarrow \gamma\gamma \end{aligned}$$

The latter process is usually neglected because of its weak cross section suppressed by a factor α_e/α_s. The photon production rate has been evaluated [18] in the case where the photon energy is large as:

$$\frac{E_\gamma dN_\gamma}{d^3p_\gamma d^4x} = \frac{2\alpha_e\alpha_s}{\pi^4}\sum_f \left(e_f^2\right)\lambda_q\lambda_{\bar{q}} T^2 \exp\left(-\frac{E_\gamma}{T}\right)\sum_{n=2}^{\infty}\frac{\lambda_g^n}{(n+1)^2}\ln\left(\frac{4E_\gamma T}{k_c^2}-1-C\right). \quad (6)$$

Because the cross-section for the Compton process is dominant and since partonic matter is gluon rich (Figure 2), direct photons are predominantly produced through gluon Compton scattering.

During the pre-equilibrium phase the longitudinal momentum of the colliding partons is not yet damped into random motion, these early collisions will therefore produce the most energetic photons. The high energy end of the photon spectrum will be thus the sensitive probe of the early phase-space distribution of partons and will inform in particular on the chemical composition of partonic matter since gluons and quarks contribute differently to the production rate, as well as on the structure function, which depletion at small fractional momentum could be best studied by comparing the relative photon production in proton-proton collisions and proton-nucleus collisions.

4.2 Equilibrium photons

4.2.1 Parton gas

During the phase when partonic matter is in thermal equilibrium, photons are produced with lower transverse momentum than in the pre-equilibrium phase since the longitudinal momentum in the entrance channel has been damped into thermal motion. The basic production processes are the same as those described earlier, Compton scattering and annihilation, and they are governed by thermal quark (Fermi-Dirac) and gluon (Bose-Einstein) distributions characterized by temperature T:

$$f_{q(g)}(E) = \frac{1}{1 \pm \exp\frac{E}{T}}. \quad (7)$$

Remember that in the hot glue scenario, the chemical equilibration for gluons could be reached much earlier than the one for quarks (0.3 fm/c compared to 1 fm/c) and with temperatures two to three times larger than the quark-gluon plasma initial temperature. Therefore the rate for the production of photons combining the two considered processes has been evaluated [18] as:

$$\frac{E_\gamma dN_\gamma}{d^3p_\gamma d^4x} = \frac{\alpha_e \alpha_s}{2\pi^2} \sum_f \left(e_f^2\right) T^2 \exp\left(-\frac{E_\gamma}{T}\right) \ln\left(\frac{0.23E_\gamma}{\alpha_s T}\right). \tag{8}$$

A recent development [20] has extended the HTL expansion to the order of two-loop and introduced two additional mechanisms which then contribute to the photon production with magnitudes larger than Compton and annihilation processes:

- Bremsstrahlung:
  Bremsstrahlung photons result from the fragmentation of quark jets into a collinear photon and a quark. Its yield has been calculated and found comparable to the Compton process at RHIC energies and provides a larger contribution than Compton scattering at LHC energies. However this production may be modified when jets traverse dense partonic matter suffering a substantial energy loss. Consequently the fragmentation of the jets into photons with high transverse momenta will be inhibited. The following parametrization has been established:

$$\frac{E_\gamma dN_\gamma}{d^3p_\gamma d^4x} = \frac{8\alpha_e \alpha_s}{\pi^5} \sum_f \left(e_f^2\right) T^2 \exp\left(-\frac{E_\gamma}{T}\right) \left(J_T - J_L\right) \ln\left(2\right), \tag{9}$$

  where $J_T \approx 4.45$ and $J_L \approx -4.26$ for 2 flavors and 3 colors of quarks. For 3 flavors of quarks, $J_T \approx 4.80$ and $J_L \approx -4.52$.

- Quark annihilation after scattering:
  Obviously the annihilation of quarks into a single photon ($q + \overline{q} \rightarrow \gamma$) does not contribute to the real photon production since there is no open phase-space for this mechanism. However such a mechanism, which arises also from certain cuts in the one- and two-loop diagrams, can occur in the medium which takes care of momentum conservation. It corresponds to the annihilation of an off mass-shell quark and an anti-quark, where the off mass-shell quark is a product of an earlier scattering of another quark or gluon. The contribution of this mechanism is given by:

$$\frac{E_\gamma dN_\gamma}{d^3p_\gamma d^4x} = \frac{8\alpha_e \alpha_s}{3\pi^5} \sum_f \left(e_f^2\right) E_\gamma T \exp\left(-\frac{E_\gamma}{T}\right) \left(J_T - J_L\right). \tag{10}$$

  This mechanism is found to completely dominate the emission of direct photons (Figure 4).

4.2.2 Hadron gas

During a later stage of the collision, when matter hadronizes, soft photons stem out of the warm and expanding hadronic matter. The spectrum follows the hadron phase-space distribution with a slope given by the hadron-gas temperature. However the spectrum can be noticeably modified by a possible transverse expansion which Doppler shifts the soft photon transverse momentum to higher values. This not likely to be the case for photons from the partonic phase since it does not last long enough to feel a transverse expansion. The photon spectrum from the hadron gas might then merge into the spectrum from the partonic gas (Figure 5). Since this last phase lasts considerably longer than the partonic phase, photons from the hadron gas might outshine photons from the earlier deconfined phase. The basic production processes involve all mesons which constitute the gas. The following ones provide the largest contributions:

- Pion annihilation:

$$\begin{aligned} \pi^+ + \pi^- &\rightarrow \gamma + \rho^0 \\ \pi^\pm + \pi^0 &\rightarrow \gamma + \rho^\pm \end{aligned}$$

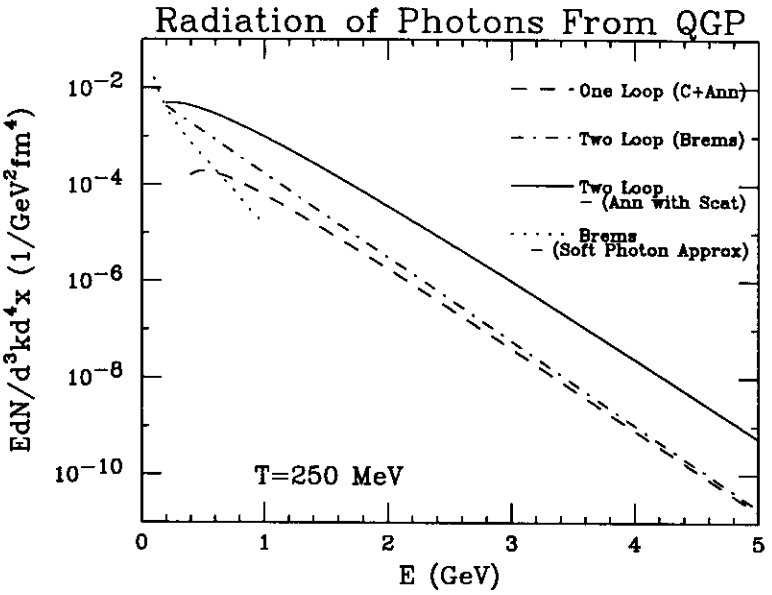

Figure 4: *Direct photon spectra radiated by an equilibrated quark-gluon plasma at a temperature of 250 MeV calculated for the various elementary processes suggested by Aurenche et al. [20] and corresponding to Equation (8) for Compton+annihilation contribution (to the order of one- and two-loop), Equation (9) for Bremsstrahlung and Equation (10) for annihilation with scattering (to the order of two-loop). From Reference [22].*

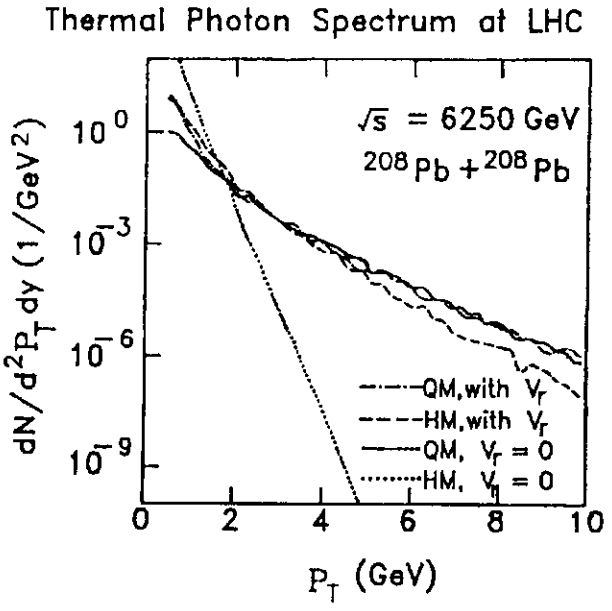

Figure 5: *Thermal photon spectrum calculated for Lead on Lead collisions at* LHC. *Contribution from the equilibrated quark-gluon plasma (*QM*) and from the hadron gas (*HM*) are displayed separately with and without (V_r = 0) transverse expansion.* QM *photons do not feel the expansion while* HM *photons are strongly Doppler shifted towards higher energies. From Reference [3].*

❒ Compton scattering:

$$\begin{aligned} \pi^{\pm} + \rho^{0} &\rightarrow \gamma + \pi^{\pm} \\ \pi^{\pm} + \rho^{\mp} &\rightarrow \gamma + \pi^{0} \\ \pi^{0} + \rho^{\pm} &\rightarrow \gamma + \pi^{\pm} \end{aligned}$$

which has been shown [21] to proceed dominantly through the a_1 resonance and to be the dominant production mechanism.

The following analytical function has been suggested to parametrize the photon production from the hadron gas [21]:

$$E_\gamma \frac{dN_{(\pi\rho \rightarrow a_1 \rightarrow \pi\gamma)}}{d\vec{p}_\gamma} = 2.4 T^{2.15} \exp\left[\frac{-1}{(1.35 T E_\gamma)^{0.77}} - \frac{E_\gamma}{T}\right]. \quad (11)$$

4.3 Total direct-photon spectrum

Folding the various photon spectra (Equations (5), (6), (8), (9), (10)) evaluated for the different production mechanisms occurring at the different stages of the collision into Equation (1), one can calculate the total spectrum for direct photons emitted during a heavy-ion collision at ultra-relativistic energies. The shape and the relative magnitude of the various components will not so much depend on the elementary production mechanism involved - although extending the calculation to higher orders can dramatically change the magnitude (see Figure 6) - but on how the collision dynamics is treated: connection between pre-equilibrium and equilibrium phase, thermal and chemical equilibrium, dynamics of the expansion ... A recent result (Figure 6) which was obtained [22] from a calculation including the elements presented in the previous sections illustrates this discussion. Pre-equilibrium photons are calculated from Compton scattering and

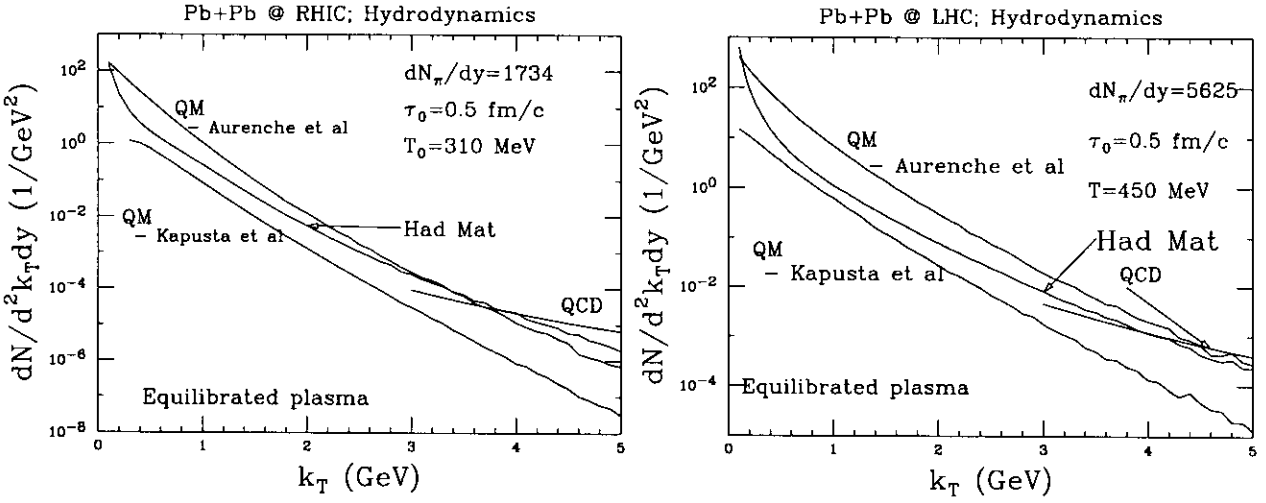

Figure 6: *Radiation of photons from central collisions of Lead nuclei at RHIC and* LHC *energies from the hadronic matter (in the mixed phase and the hadronic phase) and the quark matter (in the* QGP *phase and the mixed phase). The contribution of the quark matter (Compton scattering, annihilation, bremsstrahlung, annihilation after scattering) and those from hard* QCD *processes (Compton scattering and annihilation) are shown separately. Also an earlier calculation by Kapusta et al. [18] is shown, which includes only Compton scattering and annihilation processes. From Reference [22]*

annihilation processes exclusively and the phase-space dynamics is calculated within the Parton Cascade Model. A chemically and thermally equilibrated quark-gluon plasma is formed at $\tau_0 = 0.5$ fm/c with a temperature of 310 MeV at RHIC energies and 450 MeV at LHC energies. The critical temperature at the phase-transition is taken as $T_c = 160$ MeV and the freeze-out temperature as

T_f = 100 MeV. Photons from the equilibrated partonic gas are produced through all the two-loops processes discussed previously. The dynamics of the equilibrated phase is obtained by solving the equations of hydrodynamics including transverse expansion and three phases: quark-gluon plasma, mixed and hadronic. Photons from the partonic and the hadronic phase are displayed separately. To give an idea on the magnitude of the processes evaluated at the two-loop order by Aurenche *et al.* *[20]*, earlier calculations by Kapusta *et al.* *[18]*, which only considered a one-loop expansion, are shown for comparison. It appears clearly that without the inclusion of the two-loop processes, the hadron gas would largely outshine the light emitted by the thermal parton gas. Only in the high end of the spectrum ($E_\gamma > 4$ GeV) will pre-equilibrium QCD photons dominate over all other sources. The inclusion of bremsstrahlung and annihilation after scattering will dramatically change the picture and provide a window, up to 3 GeV at RHIC energies and beyond 4 GeV at LHC energies, where the quark-gluon plasma will shine brighter than any source.

We have discussed so far the various sources of direct photons through which one expects to gain a deep insight in the dynamic evolution of matter formed at mid-rapidity in central heavy-ion collisions at ultra-relativistic energies. We have omitted however the major contribution to the photon spectrum which completely shadows the glow of hot partonic and hadronic matter. Decay photons which originate from the two-photon decay of mainly neutral pions will blind the detectors and render direct photons hardly observable. Experimental skills will thus be necessary to dwell for the rare direct photons. To discriminate on an event-by-event basis direct photons from decay photons seems today a task out of reach even with the help of analysis based on neural networks. At variance determining the direct photon spectrum on a statistical basis, is a well established and reliable technique, provided that direct photons represent at least 5% of all produced photons. This limit is imposed by systematic errors resulting mainly from the limited phase-space covered by detectors for the detection of neutral pions.

The recent but still preliminary results (Figure 7) from the WA98 [23] collaboration indicate that, at least at SPS energies, the task of extracting direct photons has become a reasonable objective. The direct photon spectrum was obtained by subtracting from the raw photon spectrum the calculated contribution from the π^0 (98%) and η decay. This contribution was obtained from a precise measurement of the meson spectrum and an extrapolation to the full solid angle based on high-statistics simulations of pion decay.

4.4 Summary

So far we have discussed the connection between heavy-ion collisions at ultra-relativistic energies and the emission of photons (Figure 8). We claim that it is within experimental reach to eliminate on a statistical basis the photons originating from the radiative decay of long lived hadrons. Direct photons are emitted at each stage of the collision and their spectrum is characteristic of the thermodynamical state of the source where they stem from. The flash of photons coming from direct parton interactions in the collision may outshine all other photon sources at transverse momenta beyond approximately 5 GeV/c at LHC as well as at RHIC energies. The formation of a hot quark-gluon plasma will be accompanied by a second flash of thermal photons with energies lower than those of the earlier photons. Because of its possible transverse expansion the photons from the subsequent hadron gas will be observed with similar energies than the thermal QCD photons. Whether the QCD gas will shine brighter than the hadron gas depends very much on how the elementary processes are calculated. Most recent calculations indicate that the quark-gluon plasma shines much brighter (a factor 4 – 5) than the hadron gas in a momentum window which extends up to 3 – 4 GeV/c. The photon production is influenced by several parameters which could be extracted from the data, like the nuclear effects on the initial parton distribution, the dynamics of chemical and thermal equilibration ...

Accompanying QCD deconfinement, it is speculated that the high temperatures that matter reaches during heavy-ion collisions may drive the restoration of SU(3) chiral symmetry and/or U(1) symmetry. Photons can indirectly help to evidence such phenomena. The change of the neutral to charged pion ratio distribution, from Gaussian centered at a ratio of 1/3 to Bose-Einstein, signals the possible formation of a disoriented chiral condensate [24]; an enhanced production of

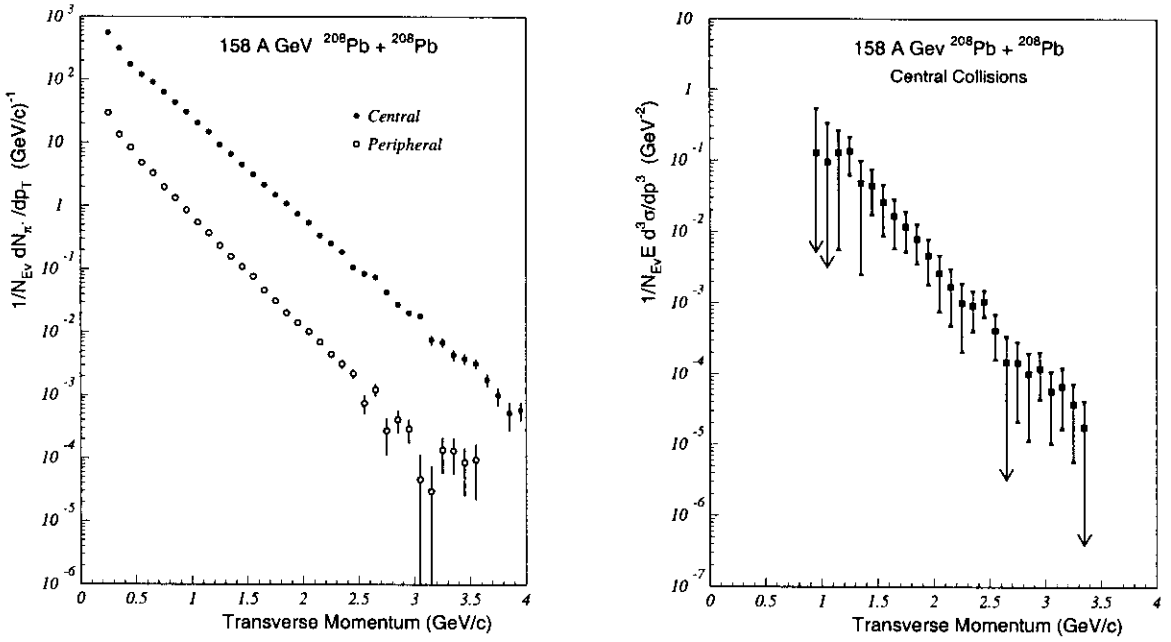

Figure 7: *Neutral pion spectrum (left) and direct photon (right) transverse energy spectrum measured by the WA98 experiment for Pb+Pb at 158A GeV. Preliminary results.*

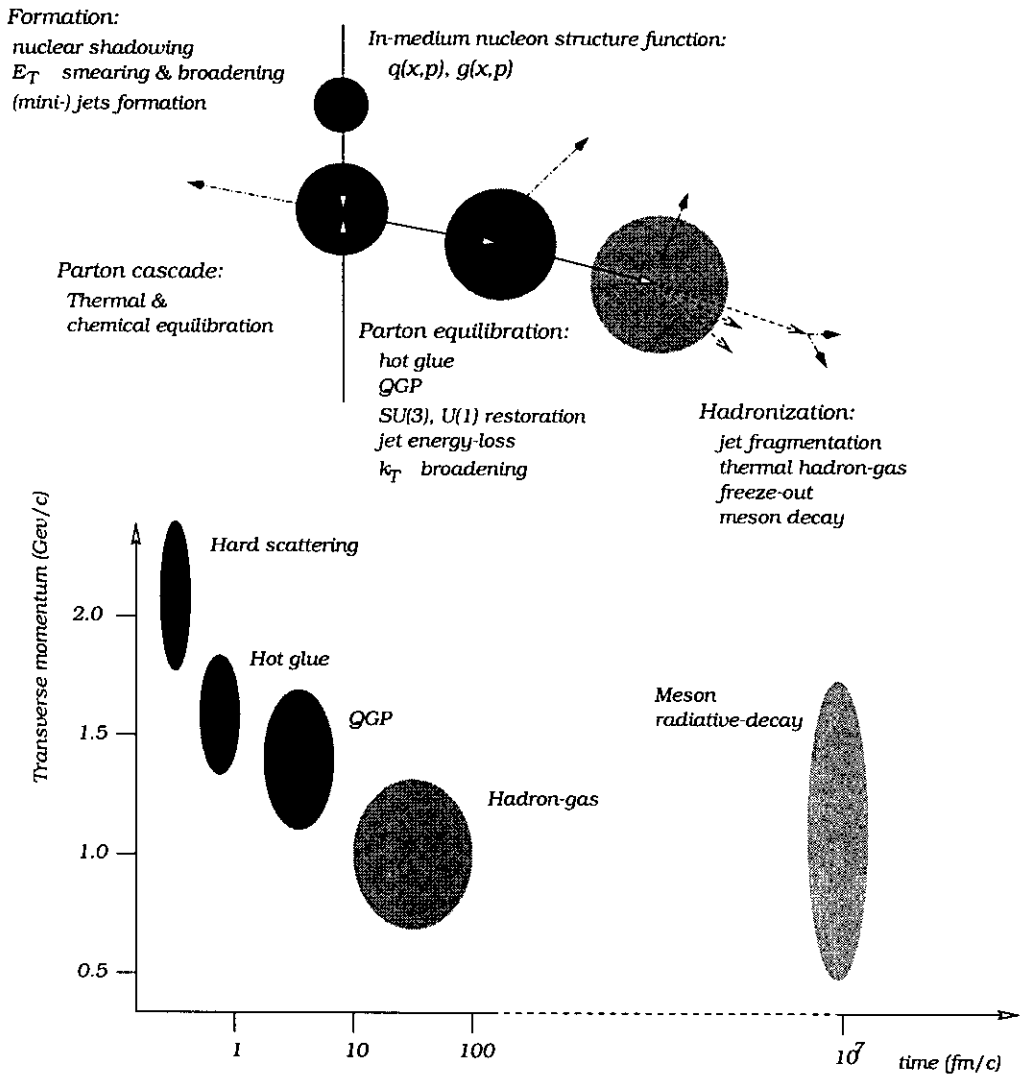

Figure 8: *A cartoon representing, as a function of their momentum and time of creation, the origin of photons emitted in a heavy-ion collision at ultra-relativistic energies. The phenomena governing the photon production are indicated. Inspired from slides by Gabor David and Paul Stankus.*

η mesons resulting from a reduction of its mass would sign U(1) symmetry restoration [25]. Such measurements will be possible with the planned detector capabilities at RHIC and LHC.

We shall now discuss what else can be learned from photons when measuring more than just their energy spectrum. The existence of the early partonic cascade can be evidenced by photon-photon interferometry and the formation of dense partonic matter by measuring the energy loss of jets tagged with photons.

5 Photon interferometry

The purpose of interferometry measurements is to distinguish the early photon component, associated to the rapidly developing parton cascade, by exploring the information on the emission time which is imprinted in the two-photon correlation pattern. I will first review the basic properties of photon statistics in quantum optics and then discuss how these properties can be used in nuclear physics [26].

5.1 Photon statistics in quantum optics

Quantum optics tells us that the statistics of photons behave differently depending on the nature of the source. In the case of a coherent source, like a laser, the number of photons measured during a time t are statistically distributed according to the Poisson law:

$$P(n) = \frac{\langle n \rangle^n}{n!} e^{-\langle n \rangle}, \tag{12}$$

where $P(n)$ is the probability to measure n photons and $\langle n \rangle$ the average number of them, measured during time t. In the case of a chaotic source, like a light bulb, which emits photons according to a Gaussian distribution and for which the coherence time, τ_c, is larger than the measurement time, the number of detected photons are distributed following a Bose-Einstein distribution:

$$P(n) = \frac{\langle n \rangle}{(1 + \langle n \rangle)^{n+1}}. \tag{13}$$

In a thermal light-source, atoms emit wave packets with a random phase-relation, i.e., incoherently. The length of such a wave packet is defined as the coherence length, L_c, and is proportional to the inverse of the spectral width of the emitted light. When the time difference between two wave packets is smaller than the coherence length, $\tau_c = L_c/c$, the packets are coherent, i.e., they have a constant phase relation.

A way to determine if a light source is a laser or a thermal source with a very narrow band width consists in measuring the second order correlation function (see for example Reference [27]). The correlation function is obtained from the probability that photons arrive in coincidence in two photon detectors, distributed as a function of the difference in arrival time, τ (Figure 9).

For a chaotic source and at coincidence time $\tau = 0$, the number of coincidences is larger than at coincidence times $\tau > \tau_c$. This can be interpreted by the fact that photons emitted by a chaotic source have the tendency to arrive in packets to the detector whereas the photon emission by a laser is regular. It is important to note that the statistics distribution is a property of the source and not of the photons.

5.2 Application to particle and nuclear physics

The property of Bose-Einstein statistics of photons can be generalized: statistical fluctuations of a chaotic system consisting of identical non-interacting bosons in the six-dimensional phase-space are not Poissonian but of Bose-Einstein type. To find at which scale the statistical behavior of identical bosons changes from a Poisson distribution to a Bose-Einstein distribution, one can, for example, measure the two-particle correlation as a function of the considered phase-space volume. This technique was first developed by Hanburry-Brown and Twiss [28] and applied to the

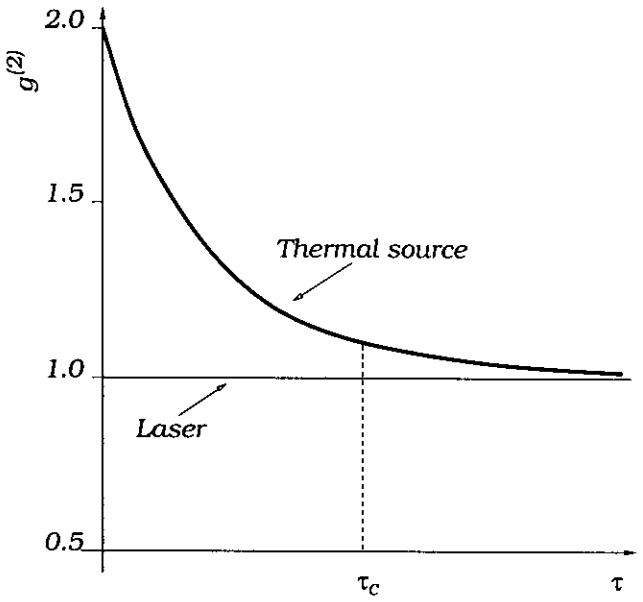

Figure 9: *Second order correlation function. For a thermal source there is an increase of the coincidence rate when the coincidence time is smaller than the coherence time. For a coherent source the correlation function remains constant and equal to 1.*

measurement of the apparent size of stars, hence the name of HBT correlations, also known as Bose-Einstein correlations (BEC). Another method consists in studying directly the count probability statistics as a function of the momentum or to study moments like factorial moments. This is the only method applicable to multi-particle correlations [29].

In particle physics the same technique was first applied by Goldhaber, Goldhaber, Lee and Pais (the GGLP effect) [30] to study the correlation between charged pions emitted in $p\overline{p}$ collisions. It has now become a common technique in particle and nuclear physics. There the space-time configuration is unknown, whereas the momentum space is accessible to measurement. The goal of a correlation measurement is to find the scale in the accessible coordinate of the phase-space for which the fluctuations become of Bose-Einstein type. The scale of the system along the unaccessible coordinates is then deduced from the phase-space volume corresponding to a single phase-space cell, $\Delta x \Delta p \sim \hbar^3$.

5.2.1 The correlation function

The two-particle correlation function is experimentally constructed from the measured probability to detect in coincidence the two particles with four-momentum k_i relative to the probability of observing the particles individually:

$$C_2(k_1, k_2) = \frac{P(k_1, k_2)}{P(k_1)\,P(k_2)}. \tag{14}$$

The denominator can be measured but is usually calculated by applying to the numerator the event-mixing technique. For an extended chaotic source the correlation function for identical non-interacting bosons is directly related to the Fourier transform of the density distribution for the particle emitting source:

$$C_2(k_1, k_2) = 1 + |\widetilde{\rho}(q; k_1 k_2)|^2. \tag{15}$$

The source density is usually parametrized in the form of a three-dimensional Gaussian distribution in the spatial coordinate and one-dimensional distribution in the time coordinate:

$$\rho(x;k_1k_2) = \frac{\mathcal{N}}{4\pi^2 R_x R_y R_z \sigma_t} \exp\left\{-\frac{x^2}{2R_x^2} - \frac{y^2}{2R_y^2} - \frac{z^2}{2R_z^2} - \frac{t^2}{2\sigma_t^2}\right\}, \tag{16}$$

which Fourier transform is:

$$\widetilde{\rho}(q;k_1k_2) = \mathcal{N} \exp\left\{-\frac{R_x^2 q_x^2}{2} - \frac{R_y^2 q_y^2}{2} - \frac{R_z^2 q_z^2}{2} - \frac{\sigma_t^2 t^2}{2}\right\}. \tag{17}$$

Combining Equations (15) and (17) the two-particle correlation function for a Gaussian source writes:

$$C_2(k_1,k_2) = C_2(q;k_1,k_2) = 1 + \mathcal{N} \exp\left(-R_x^2 q_x^2 - R_y^2 q_y^2 - R_z^2 q_z^2 - \sigma_t^2 t^2\right). \tag{18}$$

In general $\mathcal{N}, R_i$ and σ_t are parameters function of k_i. For ease of understanding we will limit the discussion to the particular case where the source is uniform, i.e., the production amplitude at various source points is independent of the source point coordinate : $\rho(x;k_1k_2) \equiv \rho(x)$, the correlation function of Equation (15) reduces to:

$$C_2(q;k_1,k_2) \equiv C_2(q) = 1 + |\widetilde{\rho}(q)|^2. \tag{19}$$

In this case the momentum correlation function is related to the Fourier transform of the space-time distribution of the source.

5.2.2 Momentum coordinates

To analyze the experimental correlation function one usually reduces the dimensionality of Equation (18) by a decomposition of the relative three-momentum $Q = k_1 - k_2$, into longitudinal (along the beam direction), $Q_L = (k_1 - k_1)$; transverse side-ward, $Q_S = Q_T \wedge k_T / |k_T|$; and transverse outward projections, $Q_O = Q_T \cdot k_T / |k_T|$; where $k_T = (k_{1_T} + k_{2_T})/2$ and $Q_T = k_{1_T} - k_{2_T}$. Within this parametrization the correlation function of Equation (18) becomes:

$$C_2(Q_S,Q_O,Q_L) = 1 + \lambda \exp\left(-Q_S^2 R_S^2 - Q_O^2 R_O^2 - Q_L^2 R_L^2\right). \tag{20}$$

For the photon-photon correlation function it is more convenient to adopt the invariant mass ($Q_{inv}^2 = (k_1 - k_2)^2 = \left(k_1^0 - k_2^0\right)^2 - \left(\overrightarrow{k_1} - \overrightarrow{k_2}\right)^2$) as the momentum coordinate because it enables to localize in limited coordinate-space decay photons from neutral pions. The correlation function then writes:

$$C_2(Q_{inv}) = 1 + \lambda \exp\left(-R_{inv}^2 Q_{inv}^2\right). \tag{21}$$

This parametrization reduces the degrees of freedom and consequently also the information since the quantity R_{inv} contains both the size of the source and its time component.

Note that in the two previous expressions of the correlation function (Equations (20) and (21)) the parameter λ reduces the amplitude of the correlation at zero relative momentum. For a fully incoherent photon-source $\lambda = 0.5$ because photons with different polarization are not identical particles anymore. The correlation can further drop when the source is partially incoherent or because of experimental artifacts like random coincidences, for example.

5.2.3 Photon-photon correlation

The two-photon correlation function is certainly the easiest to understand since photons are not subject to final-state interaction. However it is also at the same time the most difficult to measure for many reasons: direct photons are rarely produced, the overwhelming background of decay photons makes the correlation signal extremely weak, the conversion of photons into two electrons

will populate the correlation function at small relative momenta, finally photons are emitted during all stages of the collision introducing complexity in the interpretation of the correlation function. Yet the last remark can be taken positively. Indeed, at variance with hadrons which probe the system at freeze-out, photons carry information on the pre-equilibrium partonic phase, the fully equilibrated quark-gluon plasma, the phase transition or mixed phase and the hadronic matter.

An ideal two-photon correlation for a single fully incoherent source would look like the one sketched in Figure 10.

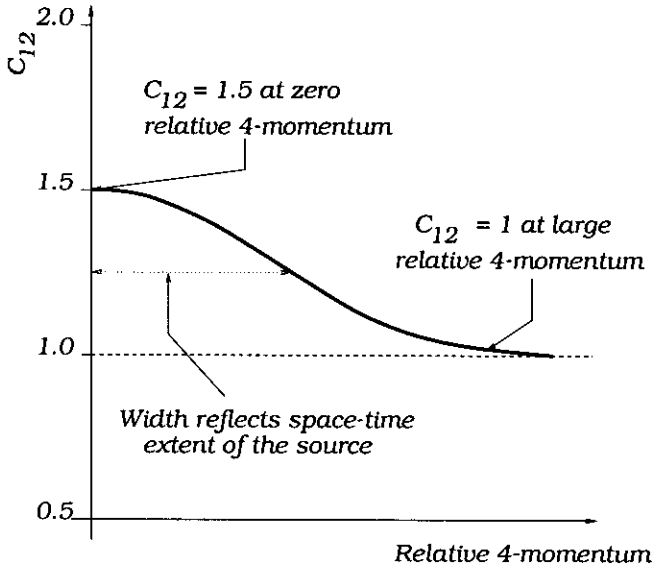

Figure 10: *Idealized two-photon correlation function. The magnitude of the correlation is limited to* $\lambda = 0.5$ *to take into account the polarization of photons.*

For photons produced during the ultra-relativistic collision, including the time dependent photon sources a more general covariant form of the correlation function has been derived [31]:

$$C_2(k_1, k_2) = \int d^4x_1 d^4x_2 w\left(x_1, \frac{k_1 + k_2}{2}\right) w\left(x_2, \frac{k_1 + k_2}{2}\right) \cos\left(\Delta x^\mu \Delta k_\mu\right), \tag{22}$$

where $w(x,p)$ represents the appropriate photon production rates of Equations (5), (6), (8), and x^μ (k_μ) is the four space-time (momentum) vector describing the time-dependent photon source obtained from models describing the pre-equilibrium and equilibrium phases. Introducing several sources with different space-time characteristics will modify the ideal correlation function represented in Figure 10 in a rather complicated way [26, 31] rendering the extraction of the source parameters model dependent. Experimental artifacts, like limited phase-space coverage, random coincidences, photon conversion ... , will finally alter the correlation in a way that can however be controlled. Besides the correlation of interest among direct-photon pairs, one has also to take into account the additional correlation of decay photons.

5.2.4 Resonance decay

For π^0 and η mesons the two-photon decay contribution to the correlation function can be well identified as it is easily localized in the relative-momentum space at the rest mass of the meson. The decay of the neutral K meson, $K_s^0 \to \pi^0\pi^0 \to \gamma\gamma\gamma\gamma$, can be also localized but it only carries a correlation which slightly modifies the two-photon correlation function for small source sizes.

5.2.5 Residual $\pi^0 - \pi^0$ correlations

Since most of the photons originate from π^0 decay, the two-photon correlation may also carry a residual correlation since pions will be themselves correlated. This can be turned to our advantage.

It is within the present identification techniques impossible to identify neutral pions on an event by event basis and consequently impossible to construct the correlation function. It was discussed [32] if the pion correlation could indeed be extracted from the measured photon correlation which writes:

$$C_{\gamma\gamma}(\Delta) = \frac{\int F_\pi(k_1)\, F_\pi(k_2)\, C_{\pi\pi}(0.5\,|k_1 - k_2|)\, d\rho}{\int F_\pi(k_1)\, F_\pi(k_2)\, d\rho}, \tag{23}$$

with the following definitions: k_i is the four-momentum of the pion which decays into two photons of momentum k_{i1} and k_{i2}, $\Delta = 0.5\,(k_{i1} - k_{i2})$ is parallel to z and $s = k_{i1} + k_{i2}$, $C_{\pi\pi}$ is the two-pion correlation function and the volume cell is:

$$\begin{aligned} d\rho \;=\; & d^3k_1 d^3k_2 d^3s \times \delta\left(\sqrt{m^2 + k_1^2} - \left|\frac{1}{2}s - \Delta\right| - \left|k_1 + \Delta - \frac{1}{2}s\right|\right) \\ & \times\delta\left(\sqrt{m^2 + k_2^2} - \left|\frac{1}{2}s - \Delta\right| - \left|k_2 - \Delta - \frac{1}{2}s\right|\right), \end{aligned} \tag{24}$$

where the δ functions ensure energy conservation at the decay vertex. Having measured the two-photon correlation function, it is sufficient to inverse the integral in Equation (23) to obtain the two-pion correlation function. This can only be done numerically. It is worth the effort because π^0 are a much better probe than the commonly used charged pions as they are not affected by the time-dependent Coulomb field in the expanding system which modifies the charged pion correlation function in a rather uncontrolled way .

5.2.6 Direct photons

As we have learned so far, direct photons have various origins with rather different source parameters. For simplicity we shall distinguish two sources only: an early one in which photons are produced in the initial parton cascade leading to thermalization of a quark-gluon plasma, and a later one where photons are radiated from thermalized matter with a phase transition. Within this photon production dynamics the two-photon correlation function is an unique tool to evidence the early perturbative QCD phase. Indeed the early emitted photons are Bose-Einstein correlated over a wide longitudinal momentum scale, thanks to their prompt emission time: $\Delta\tau = 0.5$ fm/c $\Rightarrow \Delta E = 0.4$ GeV. All other photons that emerge later are correlated at progressively narrower longitudinal momentum scales, which provides a possibility to distinguish the contribution of the early photons and to verify the existence of the predicted rapidly developing parton cascade. This effect is clearly visible in calculations performed [31, 34] for heavy-ion collisions at RHIC and LHC energies. To obtain the result displayed in Figure 11 for Lead on Lead collisions at LHC energy, the photon production dynamics was separated into two components: early photons emerging at time 0.3 fm/c from the rapidly developing parton cascade with 750 MeV effective temperature, and late photons comprising the ulterior emitted direct photons and the decay photons. It is further assumed that the fraction of the early direct photons is 5% of the total photon yield. The two-photon correlation as a function of the relative longitudinal momentum has been simulated with a longitudinal effective length of 0.3 fm. The transverse effective radius was set to 3 fm which corresponds to the *transverse* size of the colliding Pb nuclei. Gaussian shape has been assumed in the three dimensions with a maximum value of 1.5 at zero relative momentum. To enrich the selection of events with photons originating from the pre-equilibrium phase of the collision, a transverse momentum threshold of 2 GeV/c was applied to the photon energies. The expected wide HBT correlation in Q_L (Figure 11) owing to early photons is indeed seen. It extends well beyond the enormous correlation due to the two-photon decay of neutral pions. Selecting photons with lower transverse momentum, i.e. enriching the data set with photons from the equilibrium partonic and hadronic phases would narrow the correlation down to $Q_L < 0.2$ GeV/c (See Reference [31]) and render it unobservable because of the presence in the same domain of the π^0 resonance.

As a general conclusion, one can state that if during heavy-ion collisions a parton cascade phase takes place, it should be seen in the two-photon correlation function along the longitudinal dimension on a wide scale well beyond the π^0 correlation peak but only for large transverse

momentum photons which mainly originate from the pre-equilibrium phase. It should vanish for lower transverse momenta. On a shorter scale the two-photon correlation mixes correlation among photons from the equilibrium phase and residual correlations from $\pi^0 - \pi^0$ correlation. This part of the spectrum will be difficult to interpret.

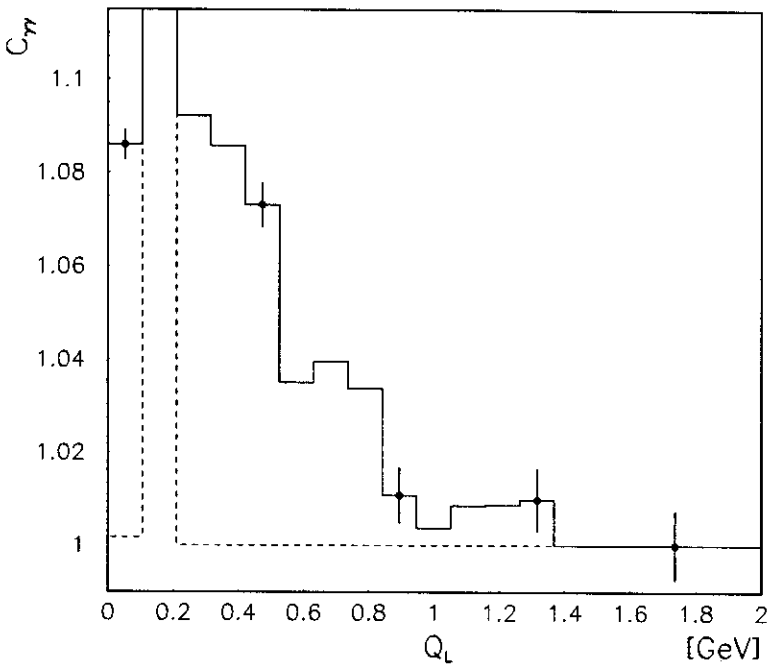

Figure 11: *Two-photon correlation function as a function of the longitudinal relative momentum with a transverse momentum cut at 2 GeV/c and $Q_S < 0.1$ GeV/c, $Q_O < 0.1$ GeV/c. Full line: $R_L = 0.3$ fm, $R_S = R_O = 3$ fm. Dashed line: the early photon component is shifted to later times by setting $R_L = 6$ fm, the resulting correlation is hidden by the pion peak which appears as a sharp peak at $Q_L = 0.135$ GeV . From Reference [34].*

6 Photon tagged jets

Understanding how single quarks and gluons propagate through hot and dense nuclear matter can inform on the nature and density of matter since the propagation in partonic matter is expected to be different than in hadronic matter. This propagation can be studied by observing, through the measurement of energy loss and direction modification, the fate of fast partons or jets, produced in the first hard collisions. Indeed the dense partonic medium modifies the initial transverse momentum of the primitive parton following the radiative emission of gluons. This results in a transverse momentum broadening and in an effective jet-energy quenching. However, in the environment of a nucleus-nucleus collision, the traditional analysis of hadronic jets is problematic. Studying high-p_t particles offers an alternative. Typically one will measure high-p_t hadron spectra and explore modifications with changing entrance channel conditions, like *p*+*A* versus *A*+*A*. Neutral mesons, π^0 and η, spectra, which can be measured with photon spectrometers up to rather high transverse momenta [33], are of particular interest for such a study. Another approach consists in searching alterations of the photon spectrum at high transverse-momentum. Indeed the direct-photon distribution is not modified by the medium but the decay-photon distribution is, since the parent neutral pions fragmented from a fast parton will be quenched. This effect decreases the photon yield (Figure 12) by a factor of about 10 at RHIC energies and 3 at LHC energies [35]. However

the interpretation of the observed quenching in terms of energy loss or mean free-path of the fast partons is far from being straightforward because the observed hadrons cannot be unambiguously be identified as belonging to a jet. One therefore ignores the original energy and momentum of the parton which has fragmented into hadrons of a given energy and one mixes hadrons in fast jets and mini-jets. Consequently the effect can be studied only qualitatively from a measurement of transverse-momentum distributions. To overcome the difficulty of not knowing precisely the jet four-momentum, it was suggested [36] to tag the energy of jets with direct photons, as a jet always accompanies a direct photon.

To proceed, one measures a photon with transverse energy E_T^γ in a given rapidity range Δy around central rapidity and at a given azimuthal angle ϕ. The p_T distribution of hadrons is then measured in the opposite direction of the kinematical region $(\Delta y, \Delta\phi)$ where one expects to find the hadrons having fragmented from the jet associated to the detected photon. Such measurements must first be done in *pp* and *pA* collisions where a dense partonic system is not expected to be formed. From *pp* collisions one investigates initial and final state interactions which cause an imbalance in the transverse energy of the photon and associated jet and a modification of the jet profile or transverse momentum smearing. Going from *pp* to *p*A (or alternatively to peripheral *AA* collisions) one adds nuclear effects in the initial and final state interactions which change the initial parton distribution in fractional momentum space and broaden the transverse momentum distribution of partons. Finally in *AA* collisions, the fractional momentum distribution of hadrons within a jet is additionally modified by the energy loss of a fast parton traveling through the dense partonic medium. The energy of the tagging photon must be selected to make sure that the average number of jets with energy $E_T = E_T^\gamma$ is less than one to avoid mixing jets with different energies. This fixes a threshold for photon energies of 15 GeV at RHIC energies and 40 GeV at LHC energies. One still needs to subtract from the hadron spectrum measured in the opposite direction of the photons, the background obtained from non photon-tagged hadrons measured in the same kinematical region. The fragmentation function can then be extracted as a function of the fractional energy $z = E_T^{hadron}/E_T^\gamma$. Finally the modifications induced by parton energy loss can be studied from the ratio of fragmentation functions obtained in *pp* and *AA* collisions. This whole procedure has been simulated [36] using the HIJING [8] event generator (Figure 13). Several

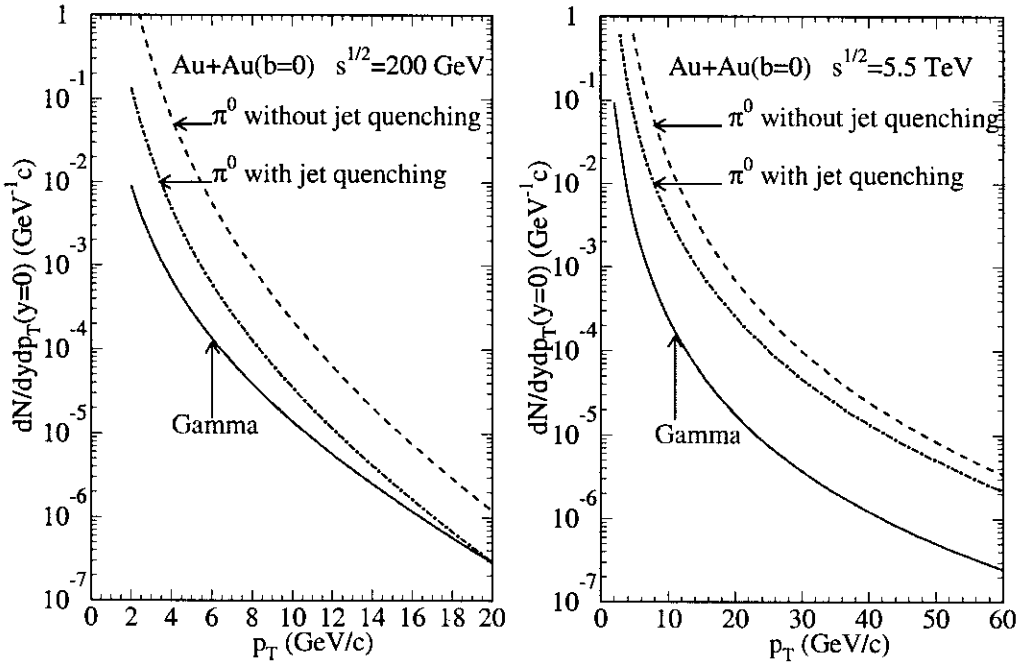

Figure 12: *The inclusive p_T distribution for π^0 with (dot-dashed) and without (dashed) parton energy loss as compared to that of direct photons (solid) in central Au+Au collisions at $\sqrt{s}$ = 200A GeV and $\sqrt{s}$ = 5.5A TeV. From Reference [36].*

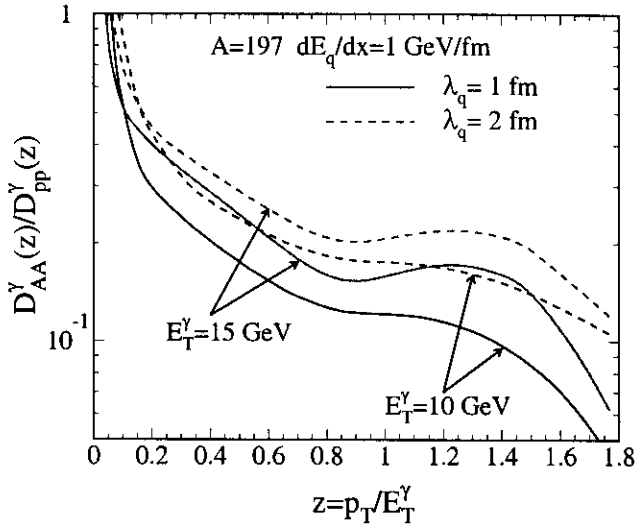

Figure 13: *The modification factors for the inclusive fragmentation function of photon-tagged jets as a function of the fractional energy calculated in central Au+Au collisions at $\sqrt{s} = 200A$ GeV for a fixed energy loss per unit distance. From Reference [36].*

features emerge from this ratio. The remaining contribution at $z \sim 1$, which originates from partons which escape the system without any scattering, provides a measure of the parton mean-free path. At intermediate z the suppression is controlled by the total energy loss and provides a measure of the parton energy loss per unit distance for fixed E_T and fixed distance through the medium.

In conclusion, observing high-p_t hadrons, preferably tagged by a high-p_t direct photon, is a method well suited to measure the energy loss of partons produced through early hard scattering and to sense the initial hot and dense environment.

7 Conclusions

The goal of ultrarelativistic heavy-ion collisions is well established: to diagnose the state of extremely hot and dense nuclear matter and seek for predicted QCD effects such as the formation of a novel state of matter, the quark-gluon plasma. How to probe this state of matter? Which observable will best *see* the first 10 fm/c of the collision? Will experiments be able to dwell the signal of interest out of the enormous background expected in heavy-ion collisions? Those remain open questions which will be addressed in the next 10 years at RHIC first and later at LHC. Among the potential signals suggested so far [1], photons and electromagnetic particles in general appear to be a very promising probe. Indeed, as any hot source of matter, nuclear matter will be characterized by a typical electromagnetic spectrum. A first flash of very energetic photons is emitted during the formation and pre-equilibrium phase through hard and semi-hard parton scattering. A second flash of softer photons will be emitted later when partonic matter has reached thermal equilibrium. While searching for these two flashes of photons one has to cope with the glow of warm hadronic matter which may shine as bright, if not brighter, than the quark-gluon plasma. Nevertheless we have seen that the latest developments in the evaluation of the QCD-photon rates predict comparatively a much dimmer hadronic spectrum. The signal conveyed by photons will arrive to the detectors quasi-unperturbed providing thus the real image of the source where they have been emitted from. This is certainly the convincing argument to search for a signal in the photon spectrum amid the technical difficulties to observe experimentally the rare direct photons among the outnumbering decay photons. Finally photons will also be very useful as messengers of the early hard-scattering to identify leading particles and to sign additional QCD events like the possible restoration of SU(3) or/and U(1) symmetries. Electromagnetic calorimeters are presently under construction, EMCAL [37] at PHENIX and PHOS [38] at ALICE. For sure exciting new physics will come out of these detectors in the coming decade.

Acknowledgements

I would like to thank my colleagues from the "Groupe Photon de subatech" [39], *Laurent Aphecteche, Hugues Delagrange, David d'Enterria, Ginés Martínez, María-Jesús Mora and Raquel Ortega*, for the enlightening daily discussions accompanying the shift of our group from low-energy to high-energy heavy-ion physics. They provided naturally a substantial help for the preparation of the present lecture and manuscript.

References

[1] S.A. Bass, M. Gyulassy, H. Stöcker, and W. Greiner, *Signatures of quark-gluon-plasma formation in high energy heavy-ion collisions: A critical review*, J. Phys. **G25**, R1 (1999).

[2] Y. Schutz, G. Martínez, F.M. Marqués, A. Marín, T. Matulewicz, R.W. Ostendorf, P. Bozek, H. Delagrange, J. Díaz, M. Franke, K.K. Gudima, S. Hlàvač, R. Holzmann, P. Lautridou, F. Lefèvre, H. Löhner, W. Mittig, M. Ploszajczak, J.H.G. van Pol, J. Québert, P. Roussel-Chomaz, A. Schubert, R.H. Siemssen, R.S. Simon, Z. Sujkowski, V.D. Toneev, V. Wagner, H.W. Wilschut and Gy. Wolf, *Hard photons and neutral pions as probes of hot and dense nuclear matter*, Nucl. Phys. **A622**, 404 (1997).

[3] J. Alam, S. Raha, and B. Sinha, *Electromagentic probes of quark-gluon plasma*, Phys. Rep. **273**, 243 (1996).

[4] S. Sarkar, *Large mass di-photons from relativistic heavy-ion collisions*, nucl-th/9704006 (1997).

[5] J.D. Bjorken, *Highly relativistic nucleus-nucleus collisions: The central rapidity region*, Phys. Rev. **D27**, 140 (1983).

[6] K.J. Eskola, *Minijets in ultrarelativistic heavy ion collisions at future colliders*, Comments Nucl. Part. Phys., **22**, 185 (1998).

[7] H.J. Drescher, M. Hladik, S. Ostapchenko, and K. Werner, *A New Approach to Nuclear Collisions at RHIC Energies*, Quark Matter'99, 14th International Conference on Ultra-Relativistic Nucleus-Nucleus Collisions, Turin, Italy; 10 - 15 May 1999.

[8] M. Gyulassy and X.-N. Wang, *HIJING 1.0: a Monte Carlo program for parton and particle production in high energy hadronic and nuclear collisions*, Comput. Phys. Commun. **83**, 307 (1994).

[9] K. Geiger and B. Müller, *Parton cascade in highly relativistic nuclear collisions*, Nucl. Phys. **A544**, 467c (1992).

[10] K. Geiger, R. Longacre and D.K. Srivastava, *VNI, simulation of high-energy particle collisions in QCD*, Comput. Phys. Commun. **104**, 70 (1997).

[11] D.K. Srivastava, M.G. Mustafa, and B. Müller, *Expanding quark-gluon plasma: Transverse flow, chemical equilibration, and electromagnetic radiation*, Phys. Rev. **C56**, (1997), 1064.

[12] E. Shuryak and L. Xiong, *Dilepton and photon production in the "hot-glue" scenario*, Phys. Rev. Lett. **70**, 2241 (1993).

[13] M. Arneodo, *Nuclear effects in structure functions*, Phys. Rep. **240**, 301 (1994).

[14] J.F. Owens, *Large-momentum-transfer production of direct photons, jets, and particles*, Rev. Mod. Phys., **59**, 465 (1987).

[15] W. Vogelsang and M.R. Whalley, *A compilation of data on single and double prompt photon production in hadron-hadron interactions*, J. Phys. **G23**, A1 (1997).

[16] C. Gale and J.I. Kapusta, *Vector dominance model at finite temperature*, Nucl. Phys. **B357**, 65 (1991).

[17] P.V. Ruuskanen, *Photons and lepton pairs: the deep probes of quark-gluon plasma*, NATO Advanced Study Institute on Particle Production in Highly Excited Matter, Castelvecchio Pascoli, Italy, 12-24 July, 1992.

[18] J. Kapusta, P. Lichard, and D. Seibert, *High energy photons from quark-gluon plasma versus hot hadronic gas*, Phys. Rev. **D44**, 2774 (1991).

[19] E. Braaten and R.D. Pisarski, *Deducing hard thermal loops from Ward identities*, Nucl.Phys. **B339**, 310 (1990).

[20] P. Aurenche, F. Gelis, H. Zaraketand R. Kobes, *Bremsstrahlung and photon production in thermal* QCD, Phys. Rev. **D58**, 85003 (1998).

[21] L. Xiong, E. Shuryak, and G.E. Brown, *Photon production through A_1 resonance in high-energy heavy-ion collisions*, Phys. Rev. **D46**, 3798 (1992).

[22] D.K. Srivastava, *Photon Production in Relativistic Heavy-Ion Collisions*, nucl-th/9904010, (1999).

[23] WA98 at CERN web pages, *http://www.cern.ch/WA98/*

[24] T.K. Nayak, WA98 Collaboration, *Present Status and Future of DCC Analysis*, Nucl. Phys., **A638**, 249c, (1998).

[25] Z. Huang and X.-N. Wang, *Partial $U(1)_A$ restoration and η enhancement in high-energy heavy-ion collisions*, Phys. Rev., **D53**, 5034 (1996).

[26] F.M. Marqués, G. Martínez, T. Matulewicz, R.W. Ostendorf, and Y. Schutz, *Two-photon correlations: From Young experiments to heavy-ion collision dynamics*, Phys. Rep. **284**, 91 (1997).

[27] R.J. Glauber, *Quantum theory of coherence* in *quantum optics* ed. S.M. Hay & A. Maitland, London, 1970.

[28] R. Hanbury-Brown, *The intensity interferometer*, Taylor & Francis Ltd., London (1974).

[29] A. Bialas, *Multiparticle* HBT *correlations*, in Proceedings of the TAPS workshop IV, *Electromagnetic and hadronic probes of nuclear matter*, edited by Y. Schutz & H. Löhner, Editions Frontières, Paris, France (1998).

[30] G. Goldhaber, S. Goldhaber, W. Lee and A. Pais, *Influence of Bose-Einstein statistics on the antiproton-proton annihilation process*, Phys. Rev. **120**, 300 (1960).

[31] A. Timmermann, M. Plumer, L. Razumov, and R.M. Weiner, *Photon interferometry of quark-gluon dynamics revisited*, Phys. Rev. **C50**, 3060 (1994).

[32] A. Deloff and T. Siemiarczuk, *Bose-Einstein correlation in a $\pi^0 - \pi^0$ system*, ALICE/98-50 Internal note (1998).

[33] M.M. Aggarwal, A. Agnihotri, Z. Ahammed, A.L.S. Angelis, V. Antonenko, V. Arefiev, V. Astakhov, V. Avdeitchikov, T.C. Awes, P.V.K.S. Baba, S.K. Badyal, A. Baldine, L. Barabach, C. Barlag, S. Bathe, B. Batiounia, T. Bernier, K.B. Bhalla, V.S. Bhatia, C. Blume, R. Bock, E.-M. Bohne, D. Bucher, A. Buijs, E.-J. Buis, Z. Böröcz, H. Büsching, L. Carlen, V. Chalyshev, S. Chattopadhyay, R. Cherbatchev, T. Chujo, A. Claussen, A.C. Das, M.P. Decowski, H. Delagrange, V. Djordjadze, P. Donni, I. Doubovik, S. Dutt, M.R. Dutta Majumdar, K. El Chenawi, S. Eliseev, K. Enosawa, P. Foka, S. Fokin, V. Frolov, M.S. Ganti, S. Garpman, O. Gavrishchuk, F.J.M. Geurts, T.K. Ghosh, R. Glasow, S.K. Gupta, B. Guskov, H.Å. Gustafsson, H.H. Gutbrod, R. Higuchi, I. Hrivnacova, M. Ippolitov, H. Kalechofsky, R. Kamermans, K.-H. Kampert, K. Karadjev, K. Karpio, S. Kato, S. Kees, B.W. Kolb, I. Kosarev, I. Koutcheryaev, T. Krümpel, A. Kugler, P. Kulinich, M. Kurata, K. Kurita, N. Kuzmin, I. Langbein, A Lebedev, Y.Y. Lee, H. Löhner, L. Luquin, D.P. Mahapatra, V. Manko, M. Martin, G. Martinez, A. Maximov, R. Mehdiyev, G.Mgebrichvili, Y.Miake, D.Mikhalev, Md.F.Mir, G.C.Mishra, Y.Miyamoto, B.Mohanty, D.Morrison, D.S.Mukhopadhyay,

V.Myalkovski, H. Naef, B.K. Nandi, S.K. Nayak, T.K. Nayak, S. Neumaier, A. Nianine, V. Nikitine , S. Nikolaev, P. Nilsson, S. Nishimura, P. Nomokonov, J.Nystrand, F.E.Obenshain, A.Oskarsson, I.Otterlund, M.Pachr, A.Parfenov, S.Pavliouk, T.Peitzmann, V.Petracek, F.Plasil, W.Pinganaud, M.L. Purschke, J. Rak, R. Raniwala, S. Raniwala, V.S. Ramamurthy, N.K. Rao, F. Retiere, K. Reygers, G. Roland, L. Rosselet, I. Roufanov, C. Roy, J.M. Rubio, H. Sako, S.S. Sambyal, R. Santo, S. Sato, H. Schlagheck, H.-R. Schmidt, Y. Schutz, G. Shabratova, T.H. Shah, I. Sibiriak, T. Siemiarczuk, D. Silvermyr, B.C. Sinha, N. Slavine, K. Söderström, N. Solomey, S.P. Sørensen, P. Stankus, G. Stefanek, P. Steinberg, E. Stenlund, D. Stüken, M. Sumbera, T. Svensson, M.D. Trivedi, A. Tsvetkov, L. Tykarski, J. Urbahn, E.C. v.d.Pijll, N. v.Eijndhoven, G.J. v.Nieuwenhuizen, A. Vinogradov, Y.P. Viyogi, A. Vodopianov, S. Vörös, M.A. Vos, B. Wyslouch, K. Yagi, Y. Yokota, G.R. Young, *Freeze-out parameters in central 158A GeV ^{208}Pb+Pb collisions*, Phys. Rev. Lett. **83**, 926 (1999).

[34] D. Ferenc, *How to test the existence of the early parton cascade using photon HBT correlations?*, 2nd Catania Relativistic Ion Studies: CRIS '98 Acicastello, Italy ; 8 - 12 Jun 1998.

[35] X.-N. Wang, *Effects of jet quenching on high p_T hadron spectra in high-energy nuclear collisions*, hep-ph/9804357 v3 (1998), and this conference.

[36] X.-N. Wang , Z. Huang, *Medium-induced parton energy loss in γ+jet events of heavy-ion collisions*, Phys. Rev. **C55**, 3047 (1997), and this conference.

[37] EMCAL, *http://www.phenix.bnl.gov/phenix/WWW/emcal/emcal.html*

[38] PHOS, Photon Spectrometer, ALICE Techinal Design Report, CERN/LHCC 99-5.

[39] GPS, *http://www-subatech.in2p3.fr/~photons*.